

Multilayered inhomogeneous beam under prescribed angle of twist and displacements: A delamination analysis

Victor I. Rizov*

*Department of Technical Mechanics, University of Architecture, Civil Engineering and Geodesy,
1 Chr. Smirnensky Blvd., 1046-Sofia, Bulgaria*

(Received December 1, 2023, Revised February 10, 2024, Accepted February 13, 2024)

Abstract. The problem considered in this theoretical paper is the delamination of a multilayered inhomogeneous beam structure that has viscoelastic behaviour under angle of twist, horizontal and vertical displacements which vary smoothly with time according to prescribed laws. The cross-section of the beam is a rectangle. The layers are made of different materials which are smoothly inhomogeneous along the length of the beam. The beam under consideration represents statically undetermined structure since it is clamped in its two ends. The problem of the strain energy release rate is solved. For this purpose, the strain energy stored in the beam structure is analyzed. In order to verify the solution obtained, the strain energy release rate is found also analyzing the time-dependent compliances of the beam under prescribed angle of twist and displacements. A parametric investigation is carried-out by applying the solution obtained. Special attention is paid to the effect of the parameters which control the variation of the angle of twist and the displacements with time on the strain energy release rate.

Keywords: delamination; displacement; inhomogeneous beam; multilayered material; twist

1. Introduction

Finding of effective solutions in structural design frequently is linked with use of modern engineering materials like, for example, the continuously inhomogeneous materials. The properties of these materials vary smoothly along one or more coordinates in the solid. The strong interest in continuously inhomogeneous materials has been stimulated by the quick development of the functionally graded materials in the recent decades (Al-Shabille *et al.* 2022, Butcher *et al.* 1999, Calim, 2020, Emad Kadum *et al.* 2021, Gasik 2010, Han *et al.* 2001, Hedia *et al.* 2014, Hirai and Chen 1999, Mahamood and Akinlabi 2017). The functionally graded materials can be classified as continuously inhomogeneous composites (El-Galy *et al.* 2019, Calim and Cuma 2022, Calim and Cuma 2023, Saiyathibrahim *et al.* 2016, Shrikantha and Gangadharan 2014). A functionally graded material has two or more constituent materials which are continuously mixed during the manufacturing process (Nemat-Allal *et al.* 2011, Toudehdehghan *et al.* 2017). The continuous variation of the microstructure and material properties in a functionally graded structural member

*Corresponding author, Professor, E-mail: V_RIZOV_FHE@UACG.BG

is controlled technologically in order to get maximum benefit from the material inhomogeneity (Hung *et al.* 2023, Hung *et al.* 2023, Markworth *et al.* 1995, Miyamoto *et al.* 1999). Recently, the application of functionally graded materials in structures and machinery in various areas of engineering has been constantly increasing (Nguen *et al.* 2023, Njim *et al.* 2021). The practice indicates that the development of such important branches of engineering as aeronautics, nuclear reactors, microelectronics, etc. owes much to use of continuously inhomogeneous (functionally graded) materials.

One of the inhomogeneous structural materials which have attracted the attention of engineers and researchers in various spheres of modern engineering are the multilayered materials. A multilayered material is a system of adhesively bonded layers. Usually, the layers are made of different materials and have different thicknesses. The basic idea of multilayered systems is to combine the properties of different materials and, in this way, to obtain a new inhomogeneous material with superior properties for a particular engineering application. The engineering practise indicates that the concept of multilayered materials represents an important tool in the rational design of a wide range of structures. The application of multilayered materials is a solution for various structural problems (for instance, reducing the weight of structures) in mechanical and civil engineering. Although the multilayered materials and structures are very modern and effective, they have some disadvantages which decrease in a high degree the beneficial effects of combining of layers of different materials in one structure. For example, multilayered structural members and components are very prone to separation of layers or delamination (Dolgov 2005, Dolgov 2016, Hutchinson and Suo 1991, Rizov 2020, 2021, Rizov and Altenbach 2022, Rizov 2022). In fact, the delamination is one of the basic factors for reducing the load-carrying capacity of multilayered structures. The delamination threatens integrity and reliability of multilayered systems and represents one of major reasons for the structural failure of multilayered engineering constructions. Thus, the safety and reliability of multilayered systems is very much dependent on their delamination behaviour. This fact indicates that if one wants to have a rational structural design approach, it would be necessary to analyze carefully different scenarios for delamination of the multilayered engineering structure under various loading conditions and external effects.

This theoretical paper is concerned with delamination analysis of a multilayered inhomogeneous beam structure with viscoelastic behaviour under angle of twist, horizontal and vertical displacements which vary smoothly with time according to prescribed laws. The layers are continuously inhomogeneous along the beam length. The cross-section of the beam is a rectangle. The beam is clamped in its both ends. Under prescribed angle of twist and displacements, the beam represents a statically undetermined structure having four degrees of indeterminacy. The main objective is to derive the strain energy release rate for the delamination. For this purpose, the strain energy stored in the beam is considered. The strain energy release rate is found also by analyzing the compliances of the beam for verification. This paper is an attempt to extent our knowledge of the multilayered inhomogeneous beam delamination problem by considering a statically undetermined viscoelastic member of rectangular cross-section subjected to combination of angle of twist, vertical and horizontal displacements. In this relation, it should be mentioned that previous delamination analyses under combined loadings deal mainly with beams of circular cross-section (Rizov 2018), while delamination studies of multilayered inhomogeneous viscoelastic beams of rectangular cross-section are focussed usually on beams under pure bending or pure torsion (Rizov 2020, 2023). Thus, this paper fills a gap in the delamination studies because the multilayered inhomogeneous beams used in the engineering practice in most of the cases have rectangular cross-section. Besides, the torsion of the multilayered beams in the engineering

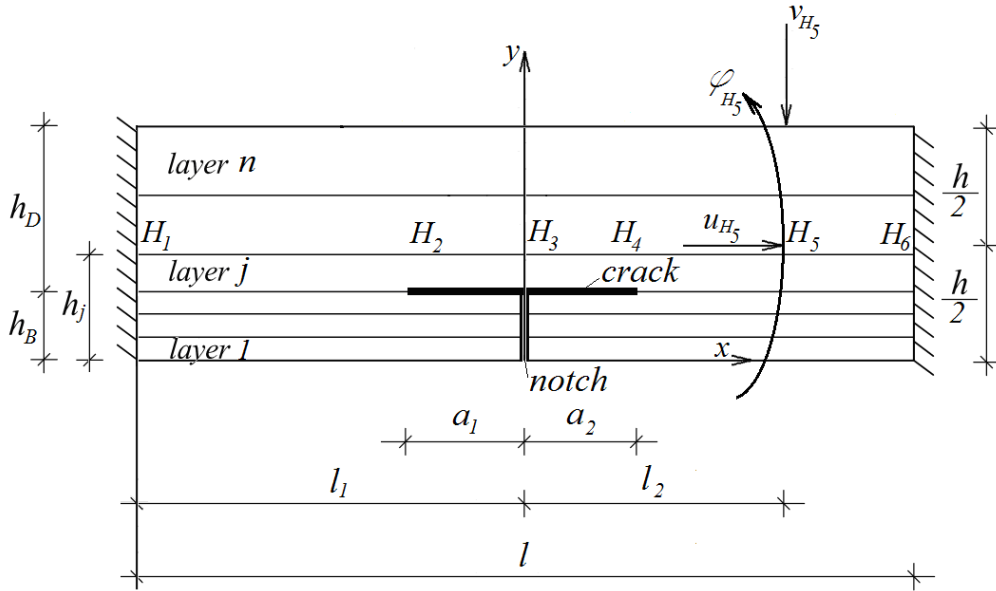


Fig. 1 Multilayered inhomogeneous viscoelastic beam structure with a delamination under prescribed angle of twist, ϕ_{H_5} , and displacements, u_{H_5} and v_{H_5}

practice frequently is in combination with bending. Both issues (rectangular cross-section and combined external loads) are addressed in this paper.

2. Theoretical model and analysis

The beam depicted in Fig. 1 consists of adhesively bonded viscoelastic layers with different thickness and material properties.

The layers exhibit continuous material inhomogeneity along the length of the beam. Besides, the number of layers is arbitrary. The cross-section of the beam is a rectangle of width, b , and thickness, h . The beam length is l . A delamination crack of length, $a_1 + a_2$, is situated in the beam as depicted in Fig. 1. The thicknesses of the lower and upper crack arms are h_B and h_D , respectively. A notch is cut-out in the lower crack arm (Fig. 1). Thus, the lower crack arm is free of stresses. The beam is loaded in section, H_5 , by external horizontal and vertical concentrated forces so as the horizontal and the vertical displacements, u_{H_5} and v_{H_5} , vary exponentially with time, t

$$u_{H_5} = \theta_1 e^{\beta t} - \theta_1, \tag{1}$$

$$v_{H_5} = \theta_2 e^{\beta t} - \theta_2, \tag{2}$$

where θ_1 , θ_2 and β are parameters controlling the variation of these displacements. Besides, the beam is loaded in torsion in section, H_5 . The angle of twist, ϕ_{H_5} , of this section varies with time according to the following exponential law

$$\phi_{H_5} = \theta_3 e^{\beta t} - \theta_3. \tag{3}$$

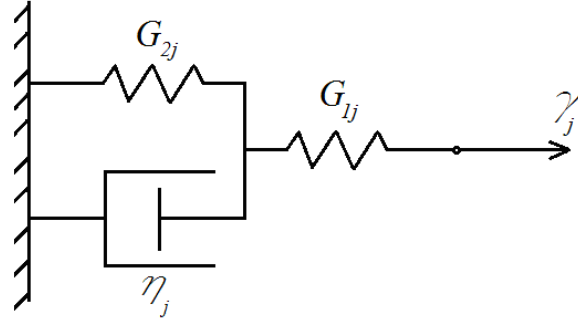


Fig. 2 Viscoelastic mechanical model

Here, θ_3 is a parameter that controls the variation of the angle of twist.

The viscoelastic behaviour of the j -th layer of the beam under torsion is treated by using the viscoelastic mechanical model depicted in Fig. 2. The shear moduli of the two springs are denoted by G_{1j} and G_{2j} (Fig. 2). The coefficient of viscosity of the dashpot is η_j (Fig. 2). The model in Fig. 2 is under shear strain, γ_j , that varies exponentially with time

$$\gamma_j = \delta_j e^{\beta \tau^t} - \delta_j, \quad (4)$$

where δ_j is a parameter. The stress-strain-time relationship of the viscoelastic model in Fig. 2 is derived in the following way.

First, the shear strain in the spring with shear modulus, G_{2j} , and in the dashpot is denoted by γ_{2j} . The shear strain in the spring with modulus of elasticity, G_{1j} , is γ_{1j} . It is obvious that

$$\gamma_{1j} + \gamma_{2j} = \gamma_j. \quad (5)$$

The shear stresses in the two springs and in the dashpot are denoted by τ_{1j} , τ_{2j} and τ_{η_j} , respectively. These shear stresses are expressed as

$$\tau_{1j} = G_{1j} \gamma_{1j}, \quad (6)$$

$$\tau_{2j} = G_{2j} \gamma_{2j}, \quad (7)$$

$$\tau_{\eta_j} = \eta_j \dot{\gamma}_{2j}, \quad (8)$$

where $\dot{\gamma}_{2j}$ is the first derivative of γ_{2j} with respect to time. The equation of equilibrium of the model is written as

$$\tau_{2j} + \tau_{\eta_j} = \tau_{1j}. \quad (9)$$

By combining of (4)-(9), one obtains the following differential equation

$$\dot{\gamma}_{2j} + \psi_{1j} \gamma_{2j} = \frac{G_{1j}}{\eta_j} (\delta_j e^{\beta t} - \delta_j), \quad (10)$$

where

$$\psi_{1j} = \frac{G_{1j} + G_{2j}}{\eta_j}. \quad (11)$$

The solution of (11) is derived as

$$\gamma_{2j} = \gamma_{2jhm} + \gamma_{2jnhm}, \quad (12)$$

where γ_{2jhm} is the solution of the homogeneous equation, γ_{2jnhm} is a particular solution of (10). The solution of the homogeneous equation is found as

$$\gamma_{2jhm} = C_C e^{-\psi_{1j}t}, \quad (13)$$

where C_C is an integration constant. The particular solution is written in the form

$$\gamma_{jnhm} = \omega_{1j}e^{\omega_{2j}t} + \omega_{3j}. \quad (15)$$

After substituting of (15) in (10), the quantities, ω_{1j} , ω_{2j} and ω_{3j} , are determined as

$$\omega_{1j} = \frac{G_{1j}\delta_j}{\eta_j(\beta^{\varpi} + \psi_{1j})}, \quad (16)$$

$$\omega_{2j} = \beta, \quad (17)$$

$$\omega_{3j} = -\frac{G_{1j}\delta_j}{\psi_{1j}\eta_j}. \quad (18)$$

The initial condition (at $t = 0$) for determination of C_C is written as

$$\gamma_{2j}(0) = 0. \quad (19)$$

By combining of (10), (12), (13), (15) and (19), one derives

$$C_C = -\omega_{1j} - \omega_{3j}. \quad (20)$$

Finally, γ_{2j} is obtained as

$$\gamma_{2j} = \omega_{1j}(e^{\beta^{\varpi}t} - e^{-\psi_{1j}t}) + \omega_{3j}(1 - e^{-\psi_{1j}t}). \quad (21)$$

From (5), one determines

$$\gamma_{1j} = \gamma_j - \gamma_{2j}. \quad (22)$$

By substituting of (21) and (22) in (6), one derives

$$\tau_{1j} = G_{1j} \left[\gamma_j - \omega_{1j}(e^{\beta^{\varpi}t} - e^{-\psi_{1j}t}) - \omega_{3j}(1 - e^{-\psi_{1j}t}) \right]. \quad (23)$$

The time-dependent shear modulus, G_{*j} , of the viscoelastic model is defined as

$$G_{*j} = \frac{\tau_{1j}}{\gamma_{1j}}. \quad (24)$$

By substituting of (4), (16), (18) and (23) in (24), one obtains

$$G_{*j} = \frac{G_{1j} \left[e^{\beta^{\varpi}t} - 1 - \frac{G_{1j}}{\eta_j(\beta + \psi_{1j})} (e^{\beta^{\varpi}t} - e^{-\psi_{1j}t}) + \frac{G_{1j}}{\psi_{1j}\eta_j} (1 - e^{-\psi_{1j}t}) \right]}{e^{\beta^{\varpi}t} - 1}, \quad (25)$$

where $j = 1, 2, \dots, n$. Here, n is the number of layers in the beam in Fig. 1. In fact, expression (25) represents the time-dependent shear modulus of the j -th layer of the beam under torsion.

Since the layers of the beam are continuously inhomogeneous along the length, the material properties, G_{1j} , G_{2j} and η_j , are distributed continuously in longitudinal direction. This distribution is described as

$$G_{1j} = G_{1Dj} e^{\rho_{1j} \frac{l_1+x}{l}}, \quad (26)$$

$$G_{2j} = G_{2Dj} e^{\rho_{2j} \frac{l_1+x}{l}}, \quad (27)$$

$$\eta_j = \eta_{Dj} e^{\rho_{3j} \frac{l_1+x}{l}}, \quad (28)$$

where

$$-l_1 \leq x \leq l - l_1. \quad (29)$$

In formulae (26)-(29), G_{1Dj} , G_{2Dj} and η_{Dj} are the values of G_{1j} , G_{2j} and η_j at the left-hand end of the beam, ρ_{1j} , ρ_{2j} and ρ_{3j} are parameters which control the distributions of G_{1j} , G_{2j} and η_j , respectively. Axis, x , is shown in Fig. 1.

The model depicted in Fig. 2 is used also to describe the viscoelastic behaviour of the j -th layer of the beam under axial forces and bending moments. Therefore, the time-dependent modulus of elasticity, E_{*j} , of the j -th layer is obtained by applying (25). For this purpose, G_{1j} , G_{2j} and η_j are replaced with E_{1j} , E_{2j} and η_{Bj} in (11) and (25). Here, E_{1j} , E_{2j} and η_{Bj} are the moduli of elasticity of the two springs and the coefficient of viscosity of the dashpot of the viscoelastic model. The distribution of E_{1j} , E_{2j} and η_{Bj} along the length is described by using (26), (27) and (28), respectively. For this purpose, G_{1Dj} , G_{2Dj} , η_{Dj} , ρ_{1j} , ρ_{2j} and ρ_{3j} are replaced by E_{1Dj} , E_{2Dj} , η_{BDj} , φ_{1j} , φ_{2j} and φ_{3j} , respectively.

The beam in (Fig. 1) is clamped at its two ends. Under the prescribed displacements and angle of twist (refer to (1), (2) and (3)), the beam has four degrees of static indeterminacy.

The static indeterminacy has to be resolved before to derive solution of the strain energy release rate for the delamination.

The horizontal and vertical reactions, R_H and R_V , and the bending and torsion moments, M_M and T_M , in the left-hand clamping are treated as redundant unknowns. The theorem of Menabrea is applied to resolve the indeterminacy

$$\frac{\partial U}{\partial R_H} = 0, \quad (30)$$

$$\frac{\partial U}{\partial R_V} = 0, \quad (31)$$

$$\frac{\partial U}{\partial M_M} = 0, \quad (32)$$

$$\frac{\partial U}{\partial T_M} = 0, \quad (33)$$

where the strain energy, U , in the beam structure is found as

$$U = U_1 + U_2 + U_3 + U_4. \quad (34)$$

Here, U_1 , U_3 and U_4 are the strain energies in beam portions, H_1H_2 , H_4H_5 and H_5H_6 , respectively. The strain energy in the upper crack arm (in beam portion, H_2H_4) is denoted by U_2 . The strain energy is calculated in the coordinate system, xy . The strain energy, U_1 , is determined as

$$U_1 = \sum_{j=1}^{j=n} \int_{-l_1}^{-a_1} \left[\iint_{(A_j)} (u_{01\tau j} + u_{01\sigma j}) dA \right] dx. \quad (35)$$

where $u_{01\tau j}$ is the strain energy density due the torsion, $u_{01\sigma j}$ is the strain energy density due the bending moment and axial force in the j -th layer of the beam, A_j is the cross-section of the layer. It should be specified that the beam has a high length to thickness ratio. Therefore, the shear stresses due to shear forces are not considered. The strain energy density, $u_{01\tau j}$, is found as

$$u_{01\tau j} = \frac{\tau_j^2}{2G^*j}. \tag{36}$$

The distribution of the shear stress, τ_j , in the cross-section of the j -th layer due to torsion is obtained by applying the formula for shear stresses in a multilayered beam loaded in torsion (Chobanian 1997)

$$\tau_j = \frac{T_M}{S_1} \left\{ \left[\sum_{k=1,3,\dots}^{\infty} (P_{k,j}ch\alpha_k y + Q_{k,j}sh\alpha_k y)\alpha_k sh\alpha_k z \right]^2 + \left[\sum_{k=1,3,\dots}^{\infty} \left(P_{k,j}sh\alpha_k y + Q_{k,j}ch\alpha_k y + \frac{8G^*j b^2}{k^3\pi^3} \right) \alpha_k \cos \alpha_k z \right]^2 \right\}^{\frac{1}{2}}. \tag{37}$$

Axis, z , is directed along the beam width at the lower surface of the beam. The quantity, α_k , is calculated as (Chobanian 1997)

$$\alpha_k = \frac{k\pi}{b}, \tag{38}$$

The quantities, $P_{k,j}$ and $Q_{k,j}$, are calculated through recurrent formulae (Chobanian 1997)

$$P_{k,j} = \frac{2}{(g_{j,j+1}-1)sh2\alpha_k h_j} \left[Q_{k,j+1}g_{j,j+1} + Q_{k,j}(sh^2\alpha_k h_j - g_{j,j+1}ch^2\alpha_k h_j) + g_{j,j+1}(r_{k,j+1} - r_{k,j})ch^{\vec{\epsilon}}\alpha_k h_j \right], \tag{39}$$

$$P_{k,j+1} = \frac{2}{(g_{j,j+1}-1)sh2\alpha_k h_j} \left[\vec{\epsilon} Q_{k,j+1}(ch^2\alpha_k h_j - g_{j,j+1}sh^2\alpha_k h_j) - Q_{k,j} + \vec{\epsilon} (r_{k,j+1} - r_{k,j})ch^{\vec{\epsilon}}\alpha_k h_j \right], \tag{40}$$

where

$$g_{j,j+1} = \frac{G^*j}{G^*(j+1)\vec{\epsilon}}, \tag{41}$$

$$r_{k,j} = \frac{8G^*j b^2}{k^3\pi^3}. \tag{42}$$

In formulae (37)-(42), $j = 1, 2, \dots, n - 1$. The quantity, h_j , is depicted in Fig. 1. Besides (Chobanian 1997)

$$P_{k,1} = -\frac{Q_{k,1}ch\alpha_k h_0 + r_{k,1}}{sh\alpha_k h_0}, \tag{43}$$

$$P_{k,n} = -\frac{Q_{k,n}ch\alpha_k h_n + r_{k,n}}{sh\alpha_k h_n}. \tag{44}$$

Equations (39), (40), (43) and (44) are used to obtain consecutively all unknowns, $P_{k,j}$ and $Q_{k,j}$, with the same index, k .

The stiffness in torsion, S_1 , involved in (37) is calculated as (Chobanian 1997)

$$S_1 = \frac{8}{\pi^2} \sum_{k=1,3,\dots}^{\infty} \frac{1}{k^2} \left\{ \frac{\alpha_k}{2} \sum_{j=1}^n r_{k,j}(h_j - h_{j-1}) + \sum_{j=1}^n P_{k,j} sh \frac{\alpha_k(h_j+h_{j-1})}{2} sh \frac{\alpha_k(h_j-h_{j-1})}{2} + \right.$$

$$+ \sum_{j=1}^n Q_{k,j} sh \frac{\alpha_k(h_j-h_{j-1})}{2} ch \frac{\alpha_k(h_j+h_{j-1})}{2} \}. \quad (45)$$

The strain energy density, $u_{01\sigma j}$, involved in (36) is found as

$$u_{01\sigma j} = \frac{\sigma_j^2}{2E^*j}, \quad (46)$$

where the normal stress, σ_j , in the j -th layer induced by the bending moment and axial force is derived as

$$\sigma_j = E^*j \varepsilon_j. \quad (47)$$

The distribution of the strains, ε_j , along the thickness is written as

$$\varepsilon_j = \kappa_1 \left(\frac{h}{2} - y - y_{n1-n1} \right), \quad (48)$$

where

$$0 \leq y \leq h. \quad (49)$$

In formula (48), κ_1 and y_{n1-n1} are the curvature and the coordinate of the neutral axis, respectively. The following equations of equilibrium are used to determine κ_1 and y_{n1-n1}

$$N_{12} = \sum_{j=1}^{j=n} \iint_{(A_j)} \sigma_j dA, \quad (50)$$

$$M_{12} = \sum_{j=1}^{j=n} \iint_{(A_j)} \sigma_j \left(\frac{h}{2} - y - y_{n1-n1} \right) dA. \quad (51)$$

The axial force, N_{12} , and the bending moment, M_{12} , in beam portion, H_1H_2 , are found as

$$N_{12} = R_H, \quad (52)$$

$$M_{12} = R_V(x + l_1) - M_M, \quad (53)$$

where

$$-l_1 \leq x \leq -a_1. \quad (54)$$

The strain energy, U_2 , is obtained as

$$U_2 = \sum_{j=1}^{j=n_1} \int_{-a_1}^{a_{21}} \left[\iint_{(A_j)} (u_{02\tau j} + u_{02\sigma j}) dA \right] dx, \quad (55)$$

where n_1 is the number of layer in the upper crack arm. The strain energy density, $u_{01\tau j}$, is determined by (36). For this purpose, n and S_1 are replaced with n_1 and S_2 in formulae (37)-(45). Here, S_2 is the stiffness in torsion of the upper crack arm (S_2 is found by replacing of n with n_1 in (45)). Formula (46) is applied to obtain $u_{02\tau j}$. For this purpose, κ_1 , y_{n1-n1} and n are replaced with κ_2 , y_{n2-n2} and n_1 in (48), (50) and (51). Besides, the bending moment involved in (51) is found as

$$M_{24} = R_V(x + l_1) - M_M + R_H \left(\frac{h}{2} - \frac{h_D}{2} \right). \quad (56)$$

The strain energy stored in beam portion, H_4H_5 , is derived as

$$U_3 = \sum_{j=1}^{j=n} \int_{a_2}^{l_2-a_2} \left[\iint_{(A_j)} (u_{03\tau j} + u_{03\sigma j}) dA \right] dx, \quad (57)$$

where $u_{03\tau j}$ and $u_{02\tau j}$ are obtained by (36) and (46). For this purpose, S_1 , κ_1 and y_{n1-n1} are

replaced with S_3 , κ_3 and y_{n3-n3} , respectively.

The strain energy, U_4 , is determined as

$$U_4 = \sum_{j=1}^{j=n} \int_{l_2}^{l-l_2} \left[\iint_{(A_j)} (u_{04\tau j} + u_{04\sigma j}) dA \right] dx. \quad (58)$$

Formulae (36) is applied to calculate $u_{04\tau j}$. For this purpose, S_1 and T_M are replaced with S_4 and T_{56} . Also, S_1 and T_M are replaced with S_4 and T_{56} in formula (37). The torsion moment, T_{56} , in beam portion, H_5H_6 , is obtained as

$$T_{56} = T_M - T_{H_5}, \quad (59)$$

where T_{H_5} is the external torsion moment applied in section, H_5 , of the beam. It should be mentioned that T_{H_5} is unknown. The strain energy density, $u_{04\sigma j}$, is calculated by (46). Equations (50) and (51) are used to determine the curvature and the coordinate of the neutral axis. For this purpose, the axial force and the bending moment in (50) and (51) are replaced by N_{56} and M_{56} . The axial force and the bending moment in portion, H_5H_6 , are derived as

$$N_{56} = R_H - F_H, \quad (60)$$

$$M_{56} = R_V(x + l_1) - M_M + F_V(x - l_2), \quad (61)$$

where F_H and F_V are the external horizontal and vertical forces applied in section, H_6 , of the beam (F_H and F_V are unknowns).

Formulae (37), (52), (53), (56), (59), (60) and (61) indicate that seven unknowns, R_H , R_V , M_M , T_M , T_{H_5} , F_H and F_V , are involved in the calculations of the strain energy in the beam structure. The same unknowns are involved also in equations (30), (31), (32) and (33). In other words, we have four equations with seven unknowns. Further three equations are composed by expressing the angle of twist, ϕ_{H_5} , and the displacements, u_{H_5} and v_{H_5} , by the theorem of Castigliano

$$\frac{\partial U}{\partial T_{H_5}} = \phi_{H_5}, \quad (62)$$

$$\frac{\partial U}{\partial F_{H^*}} = u_{H_5}, \quad (63)$$

$$\frac{\partial U}{\partial F_V} = v_{H_5}. \quad (64)$$

After substituting of the strain energy in (30), (31), (32), (33), (62), (63) and (64), the equations are solved with respect to R_H , R_V , M_M , T_M , T_{H_5} , F_H and F_V by using the MatLab computer program.

The strain energy release rate, G , at increase of delamination in the left-hand delamination tip is found as

$$G = \frac{\partial U}{b \partial a_1}. \quad (65)$$

By substituting of (34) in (65), one derives

$$G = \frac{1}{b} \left[- \sum_{j=1}^{j=n} \iint_{(A_j)} (u_{01\tau j} + u_{01\sigma j}) dA + \sum_{j=1}^{j=n_1} \iint_{(A_j)} (u_{02\tau j} + u_{02\sigma j}) dA \right]. \quad (66)$$

The material properties involved in (66) are determined at $x = -a_1$. The integrals in (66) are solved by the MatLab computer program. Formula (66) is used to obtain the strain energy release

rate at various values of time.

At increase of delamination in the right-hand delamination tip, the strain energy release rate is obtained as

$$G = \frac{\partial U}{b \partial a_2}. \quad (66)$$

By combining of (34) and (66), one determines

$$G = \frac{1}{b} \left[\sum_{j=1}^{j=n_1} \iint_{(A_j)} (u_{02\tau j} + u_{02\sigma j}) dA - \sum_{j=1}^{j=n_{\vec{\tau}}} \iint_{(A_j)} (u_{03\tau j} + u_{03\sigma j}) dA \right]. \quad (67)$$

The material properties involved in (67) are found at $x = a_2$. The integration in (67) is carried-out by the MatLab computer program. By using (67), one calculates the strain energy release rate at various values of time.

The strain energy release rate is derived also by analyzing the compliances, C_1 , C_2 and C_3 , of the beam for verification of (66) and (67). The compliances are written as

$$C_1 = \frac{u_{H_5}}{F_H}, \quad (68)$$

$$C_2 = \frac{v_{H_5}}{F_V}, \quad (69)$$

$$C_3 = \frac{\phi_{H_5}}{T_{H_5}}. \quad (70)$$

The displacements and the angle of twist are expressed as

$$\begin{aligned} u_{H_5} = & \int_{-l_1}^{-a_1} \frac{R_H}{\sum_{j=1}^{j=n_{\vec{\tau}}} E^* j A_j} \frac{R_H}{F_H} dx + \int_{-a_1}^{a_2} \frac{R_H}{\sum_{j=1}^{j=n_1} E^* j A_j} \frac{R_H}{F_H} dx + \int_{-a_1}^{a_2} \kappa_2 \frac{R_H \left(\frac{h}{2} - \frac{h_D}{2} \right)}{F_H} dx + \\ & + \int_{a_2}^{l_2} \frac{R_H}{\sum_{j=1}^{j=n} E^* j A_j} \frac{R_H}{F_H} dx + \int_{l_2}^{l-l_1-l_2} \frac{R_H - F_H}{\sum_{j=1}^{j=n} E^* j A_j} \frac{R_H - F_H}{F_H} dx, \end{aligned} \quad (71)$$

where R_H/F_H , $(R_H - F_H)/F_H$ and $R_H(h/2 - h_D/2)/F_H$ are the axial forces and the bending moment in the beam portions induced by the unit loading for determination of u_{H_5}

$$\begin{aligned} v_{H_5} = & \int_{-l_1}^{-a_1} \kappa_1 \frac{R_V(\vec{\tau} l_1 + x) - M_M}{F_V} dx + \int_{-a_1}^{a_2} \vec{\tau} \kappa_2 \frac{R_V(\vec{\tau} l_1 + x) - M_M}{F_V} dx + \\ & + \int_{a_2}^{l_2} \kappa_3 \frac{R_V(l_1 + x) - M_M}{F_V} dx + \int_{l_2}^{l-l_1-l_2} \kappa_4 \frac{R_V(l_1 + x) - M_M - F_V(x - l_2)}{F_V} dx, \end{aligned} \quad (72)$$

where $[R_V(l_1 + x) - M_M]/F_V$ and $[R_V(l_1 + x) - M_M - F_V(x - l_2)]/F_V$ are the bending moments in the beam portions induced by the unit loading for determination of v_{H_5}

$$\begin{aligned} \phi_{H_5} = & \int_{-l_1}^{-a_1} \frac{T_M}{S_1} \frac{T_M}{T_{H_5}} dx + \int_{-a_1}^{a_2} \frac{T_M}{S_2} \frac{T_M}{T_{H_5}} dx + \int_{a_2}^{l_2} \frac{T_M}{S_3} \frac{T_M}{T_{H_5}} dx + \\ & \int_{l_2}^{l-l_1-l_2} \frac{T_M - T_{H_5} \vec{\tau}}{S_4} \frac{T_M - T_{H_5}}{T_{H_5}} dx, \end{aligned} \quad (73)$$

where T_M/T_{H_5} and $(T_M - T_{H_5})/T_{H_5}$ are the torsion moments in the beam portions induced by the unit loading for determination of ϕ_{H_5} . Expressions (71), (72) and (73) are obtained by applying the integrals of Maxwell-Mohr.

By using the compliance method, the strain energy release rate at increase of the delamination in the left-hand delamination tip is found as

$$G = \frac{1}{2b} \left(F_H^2 \frac{\partial C_1}{\partial a_1} + F_V^2 \frac{\partial C_2}{\partial a_1} + T_{H_5}^2 \frac{\partial C_3}{\partial a_1} \right). \quad (74)$$

By substituting of (68), (69), (70), (71), (72) and (73) in (74), one derives

$$G = \frac{1}{2b} \left\{ -\frac{R_H^2}{\sum_{j=1}^{j=n} E^* A_j} + \frac{R_H^2}{\sum_{j=1}^{j=n_1} E^* A_j} + \kappa_2 R_H \left(\frac{h}{2} - \frac{h_D}{2} \right) - \right. \\ \left. -\kappa_1 [R_V(l_1 + x) - M_M] + \kappa_2 [R_V(l_1 + x) - M_M] - \frac{T_M^2}{S_1} + \frac{T_M^2}{S_2} \right\}. \quad (75)$$

It should be mentioned that the curvatures and the stiffness in torsion involved in (75) are obtained at $x = -a_1$. The strain energy release rates found by (75) match these determined by using (66). This fact proves the correctness of the solution of the strain energy release rate at increase of the delamination in the left-hand delamination tip.

The application of the compliance method at increase of the delamination in the right-hand delamination tip yields the following expression for the strain energy release rate

$$G = \frac{1}{2b} \left(F_H^2 \frac{\partial C_1}{\partial a_2} + F_V^2 \frac{\partial C_2}{\partial a_2} + T_{H_5}^2 \frac{\partial C_3}{\partial a_2} \right). \quad (76)$$

By combing of (68), (69), (70), (71), (72), (73) and (76), one obtains

$$G = \frac{1}{2b} \left\{ \frac{R_H^2}{\sum_{j=1}^{j=n_1} E^* A_j} + \kappa_2 R_H \left(\frac{h}{2} - \frac{h_D}{2} \right) - \frac{R_H^2}{\sum_{j=1}^{j=n} E^* A_j} + \right. \\ \left. +\kappa_2 [R_V(l_1 + x) - M_M] - \kappa_3 [R_V(l_1 + x) - M_M] + \frac{T_M^2}{S_2} - \frac{T_M^2}{S_3} \right\}. \quad (77)$$

The curvatures and the stiffness in torsion involved in (77) are derived at $x = a_2$. The fact that the strain energy release rates determined by using (77) match these obtained by (67) confirms the correctness of the analysis of the strain energy release rates at increase of the delamination in the right-hand delamination tip.

Another check-up of solutions (66) and (67) is carried-out by considering the energy balance. Eq. (78) describes the energy balance at increase of the delamination in the left-hand delamination tip.

$$F_H \delta u_{H_5} + F_V \delta v_{H_5} + T_{H_5} \delta \phi_{H_5} = \frac{\Delta U}{\Delta a_1} \delta a_1 + G b \delta a_1. \quad (78)$$

Eq. (78) is used to determine G . The result is

$$G = \frac{F_H}{b} \frac{\partial u_{H_5}}{\partial a_1} + \frac{F_V}{b} \frac{\partial v_{H_5}}{\partial a_1} + \frac{T_{H_5}}{b} \frac{\partial \phi_{H_5}}{\partial a_1} - \frac{1}{b} \frac{\partial U}{\partial a_1}. \quad (79)$$

By inserting of (34), (71), (72) and (73), one obtains

$$G = \frac{1}{b} \left\{ -\frac{R_H^2}{\sum_{j=1}^{j=n} E^* A_j} + \frac{R_H^2}{\sum_{j=1}^{j=n_1} E^* A_j} + \kappa_2 R_H \left(\frac{h}{2} - \frac{h_D}{2} \right) - \right. \\ \left. -\kappa_1 [R_V(l_1 + x) - M_M] + \kappa_2 [R_V(l_1 + x) - M_M] - \frac{T_M^2}{S_1} + \frac{T_M^2}{S_2} + \right. \\ \left. + \sum_{j=1}^{j=n} \iint_{(A_j)} (u_{01\tau j} + u_{01\sigma j}) dA - \sum_{j=1}^{j=n_1} \iint_{(A_j)} (u_{02\tau j} + u_{02\sigma j}) dA \right\}. \quad (80)$$

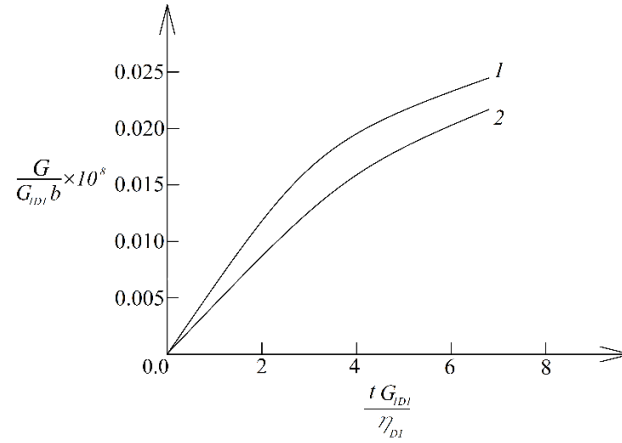


Fig. 3 The strain energy release rate versus time (curve 1-at increase of delamination in the left-hand delamination tip, curve 2-at increase of delamination in the right-hand delamination tip)

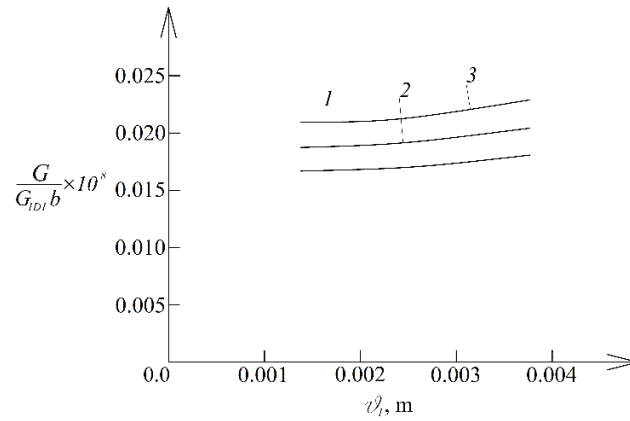


Fig. 4 The strain energy release rate versus θ_1 (curve 1-at $\rho_{11} = 0.5$, curve 2-at $\rho_{11} = 1.0$ and curve 3-at $\rho_{11} = 1.5$)

The strain energy release rates determined by (80) match these obtained by (66).

The energy balance at increase of the delamination in the right-hand delamination tip is described by Eq. (81).

$$F_H \delta u_{H_5} + F_V \delta v_{H_5} + T_{H_5} \delta \phi_{H_5} = \frac{\Delta U}{\Delta a_2} \delta a_2 + G b \delta a_2. \quad (81)$$

From (34), (71), (72), (73) and (81), it follows that

$$G = \frac{1}{b} \left\{ \frac{R_H^2}{\sum_{j=1}^{j=n_1} E^* j A_j} + \kappa_2 R_H \left(\frac{h}{2} - \frac{h_D}{2} \right) - \frac{R_H^2}{\sum_{j=1}^{j=n} E^* j A_j} + \right. \\ \left. + \kappa_2 [R_V(l_1 + x) - M_M] + \kappa_3 [R_V(l_1 + x) - M_M] + \frac{T_M^2}{S_2} - \frac{T_M^2}{S_3} - \right. \\ \left. - \sum_{j=1}^{j=n_1} \iint_{(A_j)} (u_{02\tau j} + u_{02\sigma j}) dA + \sum_{j=1}^{j=n_2} \iint_{(A_j)} (u_{03\tau j} + u_{03\sigma j}) dA \right\}. \quad (82)$$

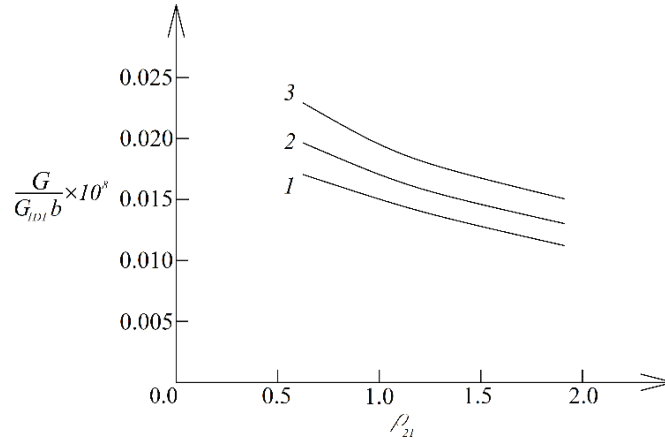


Fig. 5 The strain energy release rate versus ρ_{21} (curve 1-at $\theta_2 = 0.00066$ m, curve 2-at $\theta_2 = 0.00123$ m and curve 3-at $\theta_2 = 0.002$ m)

The strain energy release rates yielded by (82) match these generated by formula (67).

3. Parametric investigation

A parametric investigation is performed by applying the solutions of the strain energy release rate (66) and (67).

The results of the parametric investigation are presented in this section of the paper.

The following data are used: $b = 0.025$ m, $h = 0.030$ m, $l_1 = 0.300$ m, $l_2 = 0.250$ m, $l = 0.750$ m, $n = 3$, $n_1 = 2$, $\theta_1 = 0.004$ m, $\theta_2 = 0.002$ m, $\theta_3 = 0.003$ rad and $\beta = 0.3 \times 10^{-7}$ 1/s. The thickness of each layer is 0.010 m.

Fig. 3 gives the evolution of the strain energy release rate with time. It should be specified that the strain energy release rate and time in Fig. 3 are presented in non-dimensional form. For this purpose, the following formulae are applied: $G_N = G/(G_{1D1}b)$ and $t_N = tG_{1D1}/\eta_{D1}$. Fig. 3 shows that the strain energy release rate at increase of the delamination in right-hand delamination tip is lower than that that at increase of the delamination in the left-hand delamination tip.

The explanation of this is linked with the fact that the values of material properties increase from the left-hand towards the right-hand end of the beam structure.

Thus, the right-hand delamination tip is located in a beam section in which the material properties have higher values which, actually, is the reason for the decrease of the strain energy release rate.

Fig. 4 shows the results of the analysis for the strain energy release rate over parameter, θ_1 , at three values of ρ_{11} . It can be observed in Fig. 4 that increase of θ_1 induces increase of the strain energy release rate. The inspection of the curves in Fig. 4 reveals that the strain energy release rate reduces when ρ_{11} increases.

Fig. 5 presents the strain energy release rate as a function of parameter, ρ_{21} , for three values of parameter, θ_2 . One can observe in Fig. 5 that when ρ_{21} increases, the strain energy release rate reduces. The curves in Fig. 5 indicate that the strain energy release rate grows with parameter, θ_2 .

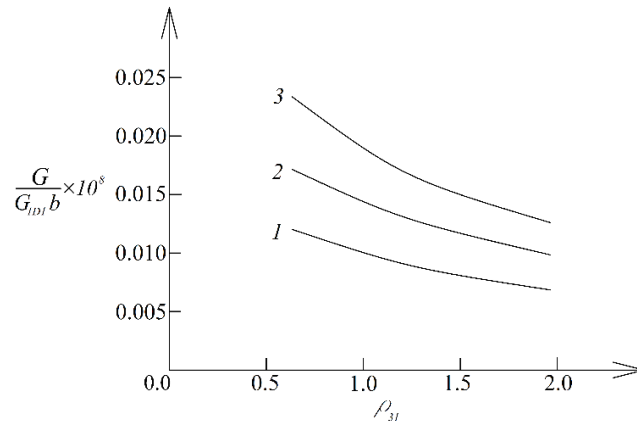


Fig. 6 The strain energy release rate versus ρ_{31} (curve 1-at $\theta_3 = 0.001$ rad, curve 2-at $\theta_2 = 0.002$ rad and curve 3-at $\theta_2 = 0.003$ rad)

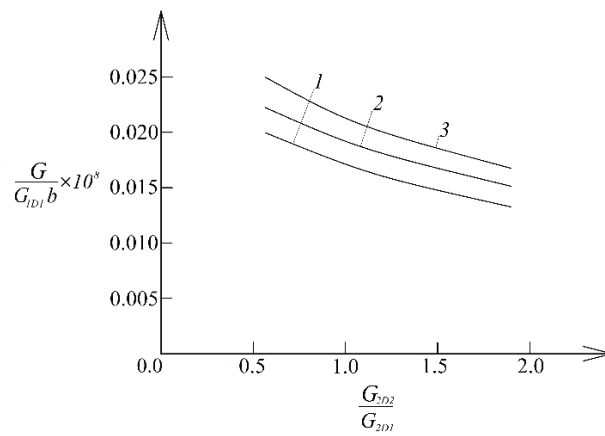


Fig. 7. The strain energy release rate versus G_{2D2}/G_{2D1} ratio (curve 1-at $\beta = 0.1 \times 10^{-7}$ 1/s, curve 2-at $\beta = 0.2 \times 10^{-7}$ 1/s and curve 3-at $\beta = 0.3 \times 10^{-7}$ 1/s)

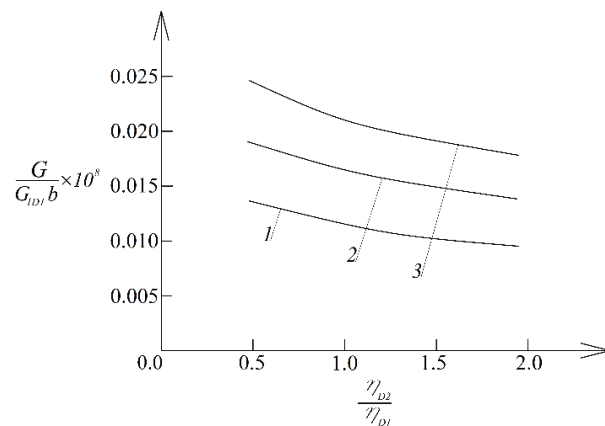


Fig. 8 The strain energy release rate versus η_{D2}/η_{D1} ratio (curve 1-at $l/h = 15$, curve 2-at $l/h = 20$ and curve 3-at $l/h = 25$)

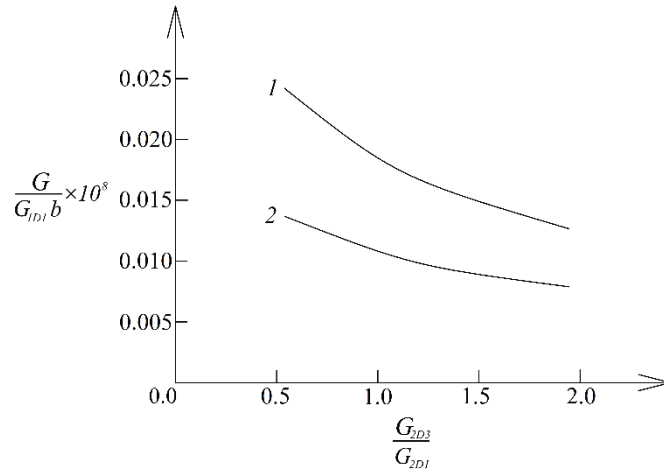


Fig. 9 The strain energy release rate versus G_{2D3}/G_{2D1} ratio (curve 1-at upper crack arm with one layer, curve 2-at upper crack arm with two layers)

The results of the investigation of the effects of parameters, ρ_{31} and θ_3 , on the strain energy release rate are shown in Fig. 6. It is evident from curves in Fig. 6 that increase of ρ_{31} causes reduction of the strain energy release rate. It can also be observed in Fig. 6 that when parameter, θ_3 , increases, the strain energy release rate increases too.

The influence of G_{2D2}/G_{2D1} ratio and parameter, β , on the strain energy release is analyzed too. In Fig. 7 the strain energy release rate is shown as a function of G_{2D2}/G_{2D1} ratio at three values of the parameter, β . It can be seen that increase of G_{2D2}/G_{2D1} ratio generates reduction of the strain energy release rate (Fig. 7). It is seen also in Fig. 7 that the strain energy release rate increases with increase of the parameter, β .

The effect of η_{D2}/η_{D1} and l/h ratios on the strain energy release rate is illustrated in Fig. 8. The curves shown in Fig. 8 indicate that the strain energy release rate reduces with increasing of η_{D2}/η_{D1} ratio. When l/h ratio increases, the strain energy release rate increases too (Fig. 8). The explanation of this behaviour is in the fact that the bending moments in the beam increase with increasing of l/h ratio.

The effect of the number of layers in the upper crack arm on the strain energy release rate is studied too. For this purpose, a three-layered beam configuration with one layer (i.e., $n_1 = 1$) in the upper crack arm and with two layers in the lower crack arm is also considered.

The strain energy release rate is plotted versus G_{2D3}/G_{2D1} ratio for both cases (upper crack arm with one layer and upper crack arm with two layers) in Fig. 9. Inspection of curves in Fig. 9 shows that the decrease of the number of layers in the upper crack arm causes significant increase of the strain energy release rate (the explanation of this finding is in the reduction of the stiffness of the upper crack arm).

4. Conclusions

Delamination of a multilayered inhomogeneous beam structure of rectangular cross-section under angle of twist, horizontal and vertical displacements which vary continuously with time

according to prescribed laws is studied by an analytical approach. The layers are continuously inhomogeneous in longitudinal direction. The beam has viscoelastic behaviour. The beam is clamped in its both ends. Therefore, under the prescribed angle of twist and displacements the beam represents statically undetermined structure having four degrees of indeterminacy. After resolving of the static indeterminacy, the strain energy release rate is obtained by considering the strain energy stored in the beam. For verification, the strain energy release rate is determined also by analyzing the compliances of the beam under prescribed angle of twist and horizontal and vertical displacements. A parametric investigation is carried-out. The results obtained indicate that the strain energy release rate reduces with increasing of the values of parameters, ρ_{11} , ρ_{21} and ρ_{31} . The increase of G_{2D2}/G_{2D1} , G_{2D3}/G_{2D1} and η_{D2}/η_{D1} ratios also generates reduction of the strain energy release rate. The explanation of these finding is linked with increase of the beam stiffness. The effect of the parameters which control the change of the prescribed angle of twist and displacements on the strain energy release rate is also assessed. It is found that increase of the values of parameters, θ_1 , θ_2 , θ_3 and β , induces increase of the strain energy release rate. The investigation reveals that when l/h ratio increases, the strain energy release rate increases too (this behaviour is due to increase of the bending moments in the beam). The analysis indicates that the strain energy release rate is influenced considerably by the number of layers in the upper crack arm. The decrease of this number generates significant increase of the strain energy release rate.

References

- Al-Shable, M., Al-Waily, M. and Njim, E.K. (2022), "Analytical evaluation of the influence of adding rubber layers on free vibration of sandwich structure with presence of nano-reinforced composite skins", *Arch. Mater. Sci. Eng.*, **116**(2), 57-70. <https://doi.org/10.5604/01.3001.0016.1190>.
- Butcher, R.J., Rousseau, C.E. and Tippur, H.V. (1999), "A functionally graded particulate composite: Measurements and failure analysis", *Acta. Mater.*, **47**(2), 259-268. [https://doi.org/10.1016/S1359-6454\(98\)00305-X](https://doi.org/10.1016/S1359-6454(98)00305-X).
- Calim, F.F. (2020), "Vibration analysis of functionally graded Timoshenko beams on Winkler-Pasternak elastic foundation", *Iran. J. Sci. Technol. Trans. Civil Eng.*, **44**(3), 901-920. <https://doi.org/10.1007/s40996-019-00283-x>.
- Calim, F.F. and Cuma, Y.C. (2022), "Vibration analysis of nonuniform hyperboloidal and barrel helices made of functionally graded material", *Mech. Bas. Des. Struct. Mach.*, **50**(11), 3781-3795. <https://doi.org/10.1080/15397734.2020.1822181>
- Calim, F.F. and Cuma, Y.C. (2023), "Forced vibration analysis of viscoelastic helical rods with varying cross-section and functionally graded material", *Mech. Bas. Des. Struct. Mach.*, **51**(7), 3620-3631. <https://doi.org/10.1080/15397734.2021.1931307>.
- Chobanian, K.S. (1997), *Stresses in Combined Elastic Solids*, Science.
- Dolgov, N.A. (2005), "Determination of stresses in a two-layer coating", *Strength Mater.*, **37**(2), 422-431. <https://doi.org/10.1007/s11223-005-0053-7>.
- Dolgov, N.A. (2016), "Analytical methods to determine the stress state in the substrate-coating system under mechanical loads", *Strength Mater.*, **48**(1), 658-667. <https://doi.org/10.1007/s11223-016-9809-5>.
- El-Galy, I.M., Saleh, B.I. and Ahmed, M.H. (2019), "Functionally graded materials classifications and development trends from industrial point of view", *SN Appl. Sci.*, **1**, 1378. <https://doi.org/10.1007/s42452-019-1413-4>
- Gasik, M.M. (2010), "Functionally graded materials: bulk processing techniques", *Int. J. Mater. Prod. Technol.*, **39**(1-2), 20-29. <https://doi.org/10.1504/IJMPT.2010.034257>.
- Han, X., Xu, Y.G. and Lam, K.Y. (2001), "Material characterization of functionally graded material by

- means of elastic waves and a progressive-learning neural network”, *Compos. Sci. Technol.*, **61**(10), 1401-1411. [https://doi.org/10.1016/S0266-3538\(01\)00033-1](https://doi.org/10.1016/S0266-3538(01)00033-1).
- Hedia, H.S., Aldousari, S.M., Abdellatif, A.K. and Fouda, N.A. (2014), “New design of cemented stem using functionally graded materials (FGM)”, *Biomed. Mater. Eng.*, **24**(3), 1575-1588. <https://doi.org/10.3233/BME-140962>.
- Hirai, T. and Chen, L. (1999), “Recent and prospective development of functionally graded materials in Japan”, *Mater. Sci. Forum*, **308-311**(4), 509-514. <https://doi.org/10.4028/www.scientific.net/MSF.308-311.509>.
- Hung, P.T., Phung-Van, P. and Thai, C.H. (2023), “Small scale thermal analysis of piezoelectric–piezomagnetic FG microplates using modified strain gradient theory”, *Int. J. Mech. Mater. Des.*, 1-23. <https://doi.org/10.1007/s10999-023-09651-y>.
- Hung, P.T., Thai, Chen H. and Phung-Van, P. (2023), “Isogeometric bending and free vibration analyses of carbon nanotube-reinforced magneto-electric-elastic microplates using a four variable refined plate theory”, *Comput. Struct.*, **287**, 107121. <https://doi.org/10.1016/j.compstruc.2023.107121>.
- Hutchinson, J.W. and Suo, Z. (1991), “Mixed mode cracking in layered materials”, *Adv. Appl. Mech.*, **29**, 63-191. [https://doi.org/10.1016/S0065-2156\(08\)70164-9](https://doi.org/10.1016/S0065-2156(08)70164-9).
- Mahamood, R.M. and Akinlabi, E.T. (2017), *Introduction to Functionally Graded Materials, Functionally Graded Materials. Topics in Mining, Metallurgy and Materials Engineering*, Springer, Cham.
- Markworth, A.J., Ramesh, K.S. and Parks, Jr. W.P. (1995), “Review: Modeling studies applied to functionally graded materials”, *J. Mater. Sci.*, **30**(3), 2183-2193. <https://doi.org/10.1007/BF01184560>.
- Miyamoto, Y., Kaysser, W.A., Rabin, B.H., Kawasaki, A. and Ford, R.G. (1999), *Functionally Graded Materials: Design, Processing and Applications*, Kluwer Academic Publishers, Dordrecht/London/Boston.
- Nemat-Allal, M.M., Ata, M.H., Bayoumi, M.R. and Khair-Eldeen, W. (2011), “Powder metallurgical fabrication and microstructural investigations of Aluminum/Steel functionally graded material”, *Mater. Sci. Appl.*, **2**(5), 1708-1718. <https://doi.org/10.4236/msa.2011.212228>.
- Nguyen, L.B., Nguyen-Xuan, H., Thai, C.H. and Phung-Van P. (2023), “A size-dependent effect of smart functionally graded piezoelectric porous nanoscale plates”, *Int. J. Mech. Mater. Des.*, **19**(4), 817-830. <https://doi.org/10.1007/s10999-023-09660-x>.
- Njim, E.K., Al-Waily, M. and Bakhy, S.H. (2021), “A critical review of recent research of free vibration and stability of functionally graded materials of sandwich plate”, *IOP Conf. Ser.: Mater. Sci. Eng.*, **1094**(1), 012081. <https://doi.org/10.1088/1757-899X/1094/1/012081>
- Njim, E.K., Bakhy, S.H. and Al-Waily, M. (2021), “Free vibration analysis of imperfect functionally graded sandwich plates: Analytical and experimental investigation”, *Arch. Mater. Sci. Eng.*, **111**(2), 49-65. <https://doi.org/10.5604/01.3001.0015.5805>.
- Rizov, V. (2018), “Analysis of cylindrical delamination cracks in multilayered functionally graded non-linear elastic circular shafts under combined loads”, *Frattura ed Integrità Strutturale*, **46**, 158-177. <https://doi.org/10.3211/IGF-ESIS.46.16>.
- Rizov, V. (2020), “Influence of the viscoelastic material behaviour on the delamination in multilayered beam”, *Procedia Struct. Integrity*, **25**, 88-100. <https://doi.org/10.1016/j.prostr.2020.04.013>.
- Rizov, V. and Altenbach, H. (2022), “Multi-layered non-linear viscoelastic beams subjected to torsion at a constant speed: A delamination analysis”, *Eng. Transac.*, **70**, 53-66. <https://doi.org/10.24423/EngTrans.1720.20220303>.
- Rizov, V.I. (2021), “Delamination analysis of multilayered beams exhibiting creep under torsion”, *Couple. Syst. Mech.*, **10**, 317-331. <https://doi.org/10.12989/csm.2021.10.4.317>.
- Rizov, V.I. (2022), “Inhomogeneous beam structures of rectangular cross-section loaded in torsion: A delamination study with considering creep”, *Procedia Struct. Integrity*, **41**, 94-102. <https://doi.org/10.1016/j.prostr.2022.05.012>.
- Rizov, V.I. (2023), “Delamination analysis of inhomogeneous viscoelastic beam of rectangular section subjected to torsion”, *Couple. Syst. Mech.*, **12**, 69-81. <https://doi.org/10.12989/csm.2023.12.1.069>.
- Saiyathibrahim, A., Subramaniyan, R. and Dhanapl, P. (2016), “Centrifugally cast functionally graded

- materials-review”, *International Conference on Systems, Science, Control, Communications, Engineering and Technology*, 68-73.
- Shrikantha Rao, S. and Gangadharan, K.V. (2014), “Functionally graded composite materials: an overview”, *Procedia Mater. Sci.*, **5**(1), 1291-1299. <https://doi.org/10.1016/j.mspro.2014.07.442>.
- Toudehdehghan, J., Lim, W., Foo1, K.E., Ma’arof, M.I.N. and Mathews, J. (2017), “A brief review of functionally graded materials”, *MATEC Web Conf.*, **131**, 03010. <https://doi.org/10.1051/mateconf/201713103010UTP-UMP>.

AI